

## Shape transition of self-assembled InAs quantum dots on GaAs(114)A

M. C. Xu, Y. Temko, T. Suzuki, and K. Jacobi\*

*Fritz-Haber-Institut der Max-Planck-Gesellschaft, Faradayweg 4-6, D-14195 Berlin, Germany*

(Received 4 June 2004; published 18 February 2005)

InAs quantum dots (QD's) grown by molecular beam epitaxy on GaAs(114)A substrates were studied by atomically resolved *in situ* scanning tunneling microscopy. Two frozen-in QD distributions prepared at different temperatures are analyzed under the assumption that QD's are depicted, which exhibit some variation in evolution mainly due to the statistics in nucleation. After nuclei formation, the QD's were found to grow in a flat form with {137} oriented facets and an aspect ratio of only 0.10. Shapes of presumably different stability were observed. During the following growth, a shape transition from flat to more steep occurs, the latter being characterized by {110} and (111)A facets and an aspect ratio of 0.20. The shape transition occurs at a critical size of the diameter which was found to be temperature dependent, i.e., 12.3 nm at 380 °C and 20 nm at 430 °C, respectively. The steep shape stays for a large size range until it is changed again. At this point both edge and screw dislocations were incorporated, which could be depicted here on top of the facets. Arguments are given that the change in critical diameter is related to In and Ga alloying and the related change in induced strain. An according growth model is proposed. Overall we conclude that the island shape derives mainly from thermodynamics rather than from kinetics.

DOI: 10.1103/PhysRevB.71.075314

PACS number(s): 68.65.Hb, 68.37.Ef, 81.05.Ea, 68.55.Ac

### I. INTRODUCTION

Three-dimensional (3D) semiconductor objects, some 10 nm in size, are able to confine electrons and holes at discrete energy levels and therefore are called quantum dots (QD's). Semiconductor QD's have attracted considerable interest recently because of their potential in technological applications.<sup>1-3</sup> QD's become self-assembled under operation of the Stranski-Krastanow (SK) growth mode (3D clusters on a wetting layer),<sup>4</sup> which occurs in heteroepitaxial systems with significant lattice mismatch, such as Ge on Si (4.2%) or InAs on GaAs (7.2%). When the amount of deposited material exceeds a critical thickness, the material in the layer(s) on top of the wetting layer accumulates into 3D clusters so that QD's are formed.

In fact, during formation the clusters or QD's will undergo a complicated evolution of their final shape, i.e., the shape is not immutable during QD evolution, but shape transitions have been found in the systems under investigation. The typical examples are Ge islands on Si(001),<sup>5-7</sup> and InAs islands on GaAs(001).<sup>8-10</sup> Atomically resolved scanning tunneling microscopy (STM) images have been reported for the shape transition of Ge QD's on Si(001) surfaces from pyramids to domes occurring at a critical base area.<sup>6</sup> InAs islands have been found to grow first in a pyramidal shape with {137} facets, corresponding to a low aspect ratio of 0.20.<sup>8-11</sup> Due to a lack in atomic resolution these facets were originally assigned to {136} ones<sup>8</sup> following Ref. 10. Saito *et al.*<sup>8</sup> found that with increasing island volume, the island shape transforms into a multifaceted one whose sides consist of {110} facets and the top facets of {136} ones, i.e., according to our believe, to {137} facets.<sup>11</sup> A similar change in shape was observed by another group.<sup>9</sup> Using ambient atomic force microscopy they evaluated the aspect ratio to change from  $\sim 0.16$  to  $\sim 0.35$  and explained this as being consistent with a change of the side walls from {136} (following Ref. 10),

i.e., from {137} to {110}. Also, for InP QD's on Ga<sub>x</sub>In<sub>1-x</sub>P two different shapes have been observed showing a surprisingly wide coexistence regime for the sizes.<sup>12</sup>

The study of the detailed behavior of QD evolution, including the shape transition, is very important both for fundamental research and for technological applications. On the one hand, it will be helpful to understand the growth mechanism; for instance, it is still debatable whether the QD shape is caused by kinetics or thermodynamics. On the other hand, it will be helpful to control the fabrication of devices with expected properties. Although the shape transition of InAs QD's grown on GaAs substrates has already been hinted in experiments,<sup>8-10</sup> to our knowledge no details of the shape evolution have been reported so far. This may be caused by difficulties in achieving atomic resolution.

For this contribution we apply atomically resolved STM and report on the evolution of InAs QD's on GaAs(114)A from small nuclei to very large dots. The structure of the GaAs(114)A surface was determined quite recently.<sup>13</sup> At temperatures above about 600 °C a stoichiometric surface can be prepared with a rather simple  $\alpha 2(2 \times 1)$  reconstruction. Under As-rich conditions at 560 °C, however, the surface becomes atomically rough and splits up into slightly tilted mesoscopic (113) and (115) facets.<sup>14</sup> Interestingly, this was not observed for the InAs wetting layer which appeared atomically disordered but flat. Also, the GaAs(114)A surface delivered reasonable sharp size distribution of InAs QD's on top of it recently.<sup>15,16</sup> Therefore, we considered the GaAs(114)A surface to be a suitable substrate for this investigation. A not too small deposition rate was adopted here in order to get QD's at different growth stages. Both flat and steep QD's, a shape transition, a critical size for the shape transition, stable and unstable QD's, and slip and screw dislocations are found during the evolution. Finally, a growth model is proposed.

## II. EXPERIMENT

The experiments were performed in a multichamber ultra-high vacuum (UHV) system as described in detail elsewhere.<sup>17</sup> Both the STM (Park Scientific Instruments, VP2) chamber and analysis chamber have base pressures better than  $1 \times 10^{-10}$  mbar, and the molecular-beam epitaxy (MBE) chamber has a base pressure better than  $2 \times 10^{-10}$  mbar with liquid  $N_2$  cooling. The samples with a typical size of  $10 \times 10$  nm<sup>2</sup> were cut from a GaAs(114) wafer (*n*-type, Si-doped, carrier concentration  $(1.4\text{--}4.8) \times 10^{18}$  cm<sup>-3</sup>, Wafer Technology). After cleaning by several ion bombardment and annealing cycles, about 30-nm-thick GaAs buffer layers were grown by MBE at a temperature of 570 °C, and then annealed for 5–8 min at the same temperature with the  $As_2$  shutter closed. The temperature was measured by a pyrometer that was calibrated against the GaAs(001)  $c(4 \times 4)$  to  $(2 \times 4)$  transition at  $465 \pm 10$  °C. Afterwards, the samples were cooled down to about 380 or 430 °C. At these temperatures InAs was deposited at a rate of  $0.08 \text{ \AA s}^{-1}$  with an  $As_2$ :In beam equivalent pressure of 70. The transition from 2D layers to 3D islands is monitored by reflection high-energy electron diffraction (RHEED) making use of the transition in the pattern from streaks to spots. In experiments, 0.33 nm [1.1 monolayer (ML)] and 0.44 nm (1.5 ML) InAs were grown at 380 and 430 °C, respectively. Here, 1 ML is defined as the monolayer thickness ( $\sim 0.3$  nm) on InAs(001). The deposition of InAs onto GaAs(114)A led to the appearance of sharp spots in the RHEED pattern (with the electron beam along  $[2\bar{2}\bar{1}]$ ), indicating the onset of 3D SK growth. After shutting off the In and  $As_2$  sources, the samples were rapidly transferred to the analysis chamber and cooled down to room temperature before STM images were acquired in constant current mode.

## III. RESULTS AND DISCUSSION

### A. Initial growth

Figure 1 shows an overview STM image of InAs islands grown on GaAs(114)A surfaces at 380 °C. Compared to the known QD ensembles, the number density is rather high, which is caused by a reasonably high deposition rate ( $0.008 \text{ nm s}^{-1}$ ) and a low growth temperature (380 °C). The low temperature decreases the mobility of the adatoms on the wetting layer, and the high deposition rate leads to fast nucleation. Islands of different size coexist indicating that they are at different growth stages. This is a basic assumption which is supported by the many results for the system studied including the present paper. The idea is that there is nucleation during a given window in time, which is certainly smaller than the total growth time but nevertheless not negligible but a fraction of, e.g., 5% to 20%. If furthermore the growth speed of a single QD is not very high, i.e., if it is of the order of the growth time of the whole ensemble, then there will be at any time a distribution of evolution states in the QD ensemble. So, one single frozen-in distribution represents also a time window in evolution. This view is quite generally accepted in QD studies.<sup>6</sup> Figure 1 comprises such a time window in which—for the given preparation temperature—

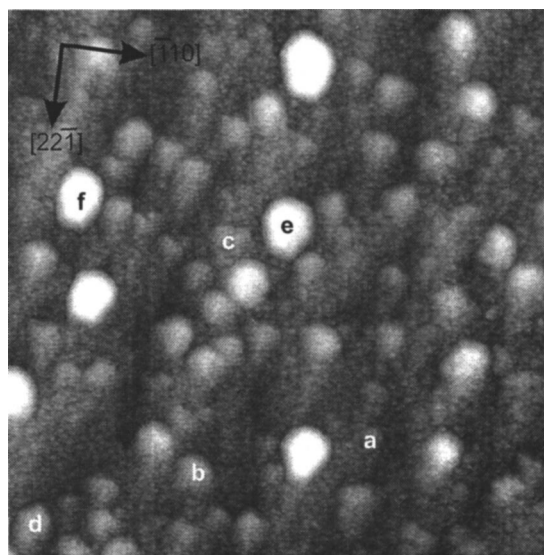


FIG. 1. Overview STM image of InAs islands on GaAs(114)A prepared at 380 °C. The image size is  $100 \times 100$  nm<sup>2</sup>. Some of the islands, whose shape is shown below in atomically resolved images, are marked.

the most advanced QD's have reached a critical diameter introduced below.

Continuing the presentation of Fig. 1, the islands can be divided into two types, a flat and a steep one. The former possesses base areas of different size while the latter grows with the same base area. Both types have  $(\bar{1}10)$  as symmetry plane, which reflects the symmetry of the underlying substrate. Some islands are marked to be further discussed below.

A height distribution was derived from Fig. 1 and is shown in Fig. 2 as a function of diameter. The diameter along the  $[2\bar{2}\bar{1}]$  direction is taken at the bottom, and the height is evaluated with respect to the wetting-layer surface. (The islands marked in Fig. 1 are indicated again.) The plot is divided into two parts, a flat one for diameters between 4 and 12.3 nm and a steep one at a diameter of 12.3 nm, i.e., the islands grow with a flat shape for some time and

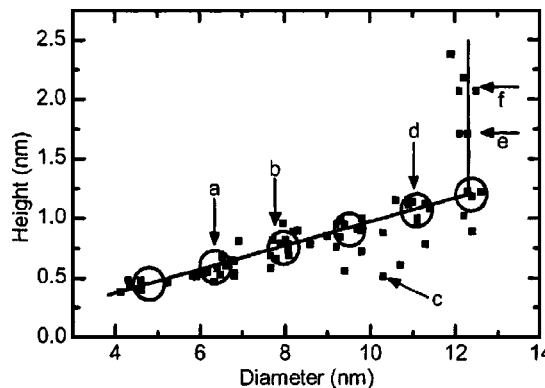


FIG. 2. Height of InAs islands as a function of their diameter. The straight lines are a guide to the eye. In the plot the positions are given for those islands, which are marked in Fig. 1 and are shown in atomically resolved images below.

suddenly—at a given diameter—change to a much steeper shape. Such a bimodal distribution is consistent with those found for InAs on GaAs(001) (Ref. 8) and Ge on Si(001) (Refs. 5 and 6). Quite obviously, Fig. 2 marks a transition of the island shape from flat to steep.

In addition, in Fig. 2 certain regions, marked by circles that were evenly spaced and then observed to fall on or near clusters of high-density points. The presence of such regions indicates that these islands are lying near stable states. The height intervals between these stable states are about 0.16 nm, an interval that is about twice the InAs (137) layer thickness of 0.079 nm. Actually, the increase in height has to be taken in the  $[114]$  direction, the amount being 0.080 nm, which is about the same. We do not have an atomic model for the growth to explain the factor of 2 but we believe that it is connected with the dimer formation at the (137) surface, which is between two neighboring As atoms lying in two neighboring (137) planes.

As shown below, the islands in the stable states have the top  $\{137\}$  layer completed. Besides the accumulation in the circles, few data do not fall into these circles. It seems that the islands are actually in an unstable state, in which the top  $\{137\}$  layer on the islands is not completed. Compared to the full layer, the incomplete top layer presumably contains atoms with more dangling bonds that increase the surface energy, making them less stable. Furthermore, the incoming atoms will find higher coordinated sites being more favorable for attachment than the sites on top of a complete layer. Both factors cause the growth to be faster at the incomplete layer than on the top of the complete layer. The faster growth rate of the unstable islands reduces their number as compared to the stable islands.

With increasing diameter (or base area), the height increases linearly. This results in a constant aspect ratio  $h/d$  of height ( $h$ ) to diameter ( $d$ ) of about 0.10. When the diameter reaches a certain value (12.3 nm here), further increase in the diameter is suddenly stopped, while the height increases further. The different growth rates for the base and the height lead to a shape transition from flat to steep while the island volume increases. Such shape transitions have also been observed for other systems.<sup>5–10</sup> Although the flat dots developing first reduce the strain, they are still strained. Therefore, it is very plausible that at a given diameter this strain is again too large, so that the lateral growth is slowed down and the dots grow mainly vertically, which then results in the shape transition.

To study the island shape in detail, Fig. 3 shows 3D STM images of some typical islands with atomic resolution. These islands have been marked already in Figs. 1 and 2. The islands in Figs. 3(a)–3(d) are in a state before and in the Figs. 3(e) and 3(f) during the shape transition. The small bulges on the facets of the islands are very likely As dimers. The formation of As dimers is the most effective means to lower the surface energy and is also very likely in view of the high As<sub>2</sub> pressure during preparation and cooling down. Furthermore, this is seen from the kind of the unit cell discussed in the following. The bulges appear with some local ordering for which surface unit cells of—strangely enough—the same size are derived as indicated in the figures. According to the angle against the substrate and the unit cell, the top facets are

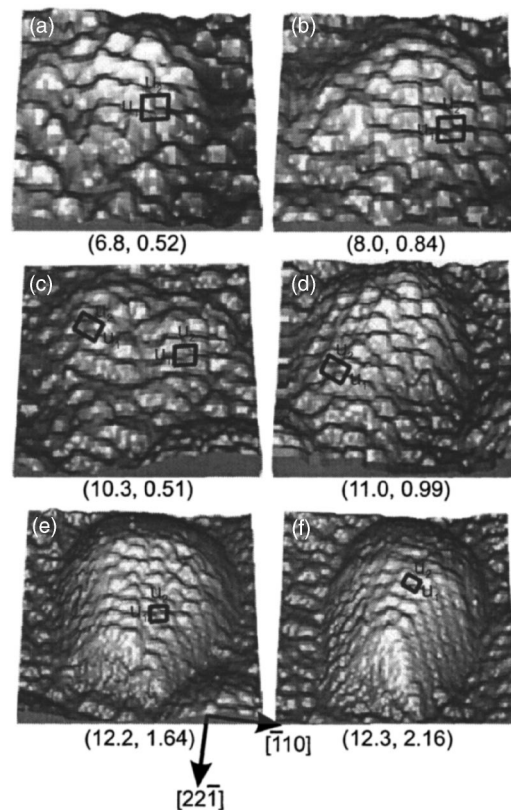


FIG. 3. Atomically resolved 3D STM images of InAs islands grown on GaAs(114)A. The diameter and height (in units of nm) of the individual QD are given in brackets at the bottom of each image. The image sizes are (a)  $7.4 \times 7.4 \text{ nm}^2$ , (b)  $7.6 \times 7.6 \text{ nm}^2$ , (c)  $9.4 \times 9.4 \text{ nm}^2$ , (d)  $10.1 \times 10.1 \text{ nm}^2$ , (e)  $12.9 \times 12.9 \text{ nm}^2$ , and (f)  $12.5 \times 12.5 \text{ nm}^2$ , respectively. The unit cells of  $\{137\}$  surfaces with unit vectors  $u_1$  and  $u_2$  are marked.

determined as  $\{137\}A$  or  $\{137\}A$ -like oriented. It is known that such  $\{137\}$  facets precede  $(2\ 5\ 11)$  facet formation.<sup>18</sup> The unit cell vectors of the top  $\{137\}A$  facets for all the islands in Fig. 3 are  $u_1=0.78 \text{ nm}$ ,  $u_2=0.98 \text{ nm}$ , and  $u_3=1.15 \text{ nm}$  within an error range of  $\pm 0.02 \text{ nm}$ . These values are consistent with those for the bulk-truncated  $\{137\}$  unit cell ( $u_1=0.742 \text{ nm}$ ,  $u_2=0.958 \text{ nm}$ , and  $u_3=1.134 \text{ nm}$ ). A change of unit cell vectors due to the anticipated strain is not observed here within our accuracy. This indicates that the strain is localized in the bottom most few layers and decays quickly with increasing height. We add that the trenched structure of the  $\{137\}$  or  $\{137\}$ -like reconstruction may be favorable for the relief of strain.

Not all facets on top of the QD's are well ordered but for convenience we call them all  $\{137\}$ . The islands in Figs. 3(a), 3(b), and 3(d) exhibit the same shape in spite of their increasing size; they are mainly terminated by the top  $\{137\}A$  facets. A shape model will be given below. The island in Fig. 3(c) seems somewhat different. In fact, this is an island just in an unstable state (see also Fig. 2); the two  $\{137\}A$  facets are rather incomplete with a dip in between rather than a peak. In contrast, the islands in Figs. 3(a), 3(b), and 3(d) are basically complete, i.e., are in a stable state (see Fig. 2). The islands shown in Figs. 3(e) and 3(f) exhibit steeper side facets with

the same base-area size but with different heights. Quite obviously, the steeper side facets, which will be shown below to belong to the  $\{110\}$  and  $(111)A$  families, emerge by stacking  $\{137\}$ -like layers as the height increases. The round vicinal (001) region (see below) increases simultaneously. No unstable island, i.e., with incomplete  $\{137\}$ -like topside facets was observed among the steep islands.

The unstable island shown in Fig. 3(c) seems to grow from the foot of the two symmetric dot sides. There exist two other types of unstable islands that are not shown here. In one case the facets grow first from the foot along the symmetry axis; in the other case the facets start growing from the top of the island. This observation is in agreement with the scatter of data points in Fig. 2. The very few data above the straight line correspond to unstable islands growing from on top whereas the data below the line correspond to those growing from the foot. The latter are more numerous than the former because the nucleation is presumably much easier at the foot than at the top of the QD.

Analyzing the deviations more quantitatively, we find that, within the error range, the deviation in height above the flat straight line in Fig. 2 is only about  $0.16 \pm 0.02$  nm, consistent with the thickness of two  $\{137\}$  layers. This means that there exists only one incomplete layer of the top facet for the third type of unstable islands. For the islands below the straight line, the deviation in height is not so uniform with a maximum at about  $0.35 \pm 0.02$  nm equivalent to a thickness of four  $\{137\}$  layers ( $\sim 0.32$  nm); before the first layer is completed at the top, a second layer already begins forming at the foot. When the base area reaches a certain value, the evolution of islands with only increasing the height but keeping the base area constant, becomes favorable. This leads to the vertical straight line in Fig. 2.

The fact that all three types of unstable islands will achieve the same stable final state with complete facets indicates that any anticipated anisotropy of the adatom diffusion on the sample surface is not critical for the shape evolution even at low temperature. The islands with complete facets are obviously lower in energy. Thus, the shape of the QD's seems to be mainly controlled by thermodynamic equilibrium.

The schematic structures for the stable—flat and steep— islands are presented in the right-hand side of Fig. 4. The corresponding 3D STM images are shown in the left-hand side. The details of the shape determination for the steep islands can be found in an earlier contribution.<sup>19</sup> The small, flat island is composed of  $\{137\}A$  facets and a small round vicinal (001) region. The steep island is composed of top  $\{137\}A$  facets,  $(111)A$  and  $\{110\}A$  side facets, and a round region. With the increase of the side facets, the top facets decrease accordingly.

Based on the structural models for islands of different volume, schematic cross sections of the growing islands are derived as shown in Fig. 5 in side view for two azimuths. After the formation of the nucleus, the island starts evolving by covering flat  $\{137\}$  facets layer by layer, with the base area and the height increasing simultaneously. During this growth stage, the aspect ratio of about 0.10 keeps the same for the stable states. Reaching a critical value the base area stops increasing, and only the height increases by stacking

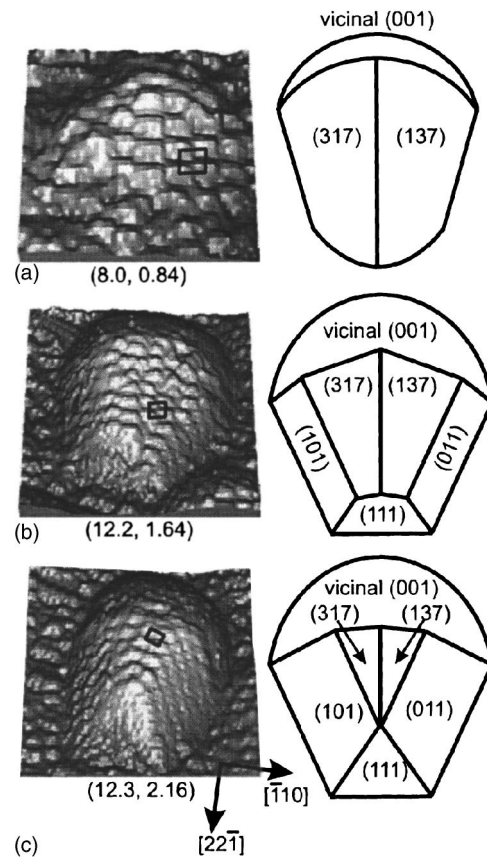


FIG. 4. Schematic structure models of the QD's at right-hand side. The corresponding original STM images are shown at the left-hand side. The diameter and height (in units of nm) of the individual QD are given in brackets at the bottom of each image. The image sizes are (a)  $7.6 \times 7.6$  nm<sup>2</sup>, (b)  $12.9 \times 12.9$  nm<sup>2</sup>, and (c)  $12.5 \times 12.5$  nm<sup>2</sup>, respectively.

$\{137\}$  layers, thus forming  $\{110\}$  and  $(111)A$  side facets. During this shape transition, the aspect ratio is raised up to a maximum value of about 0.20 and is kept constant then during the further growth. This growth model with an inherent

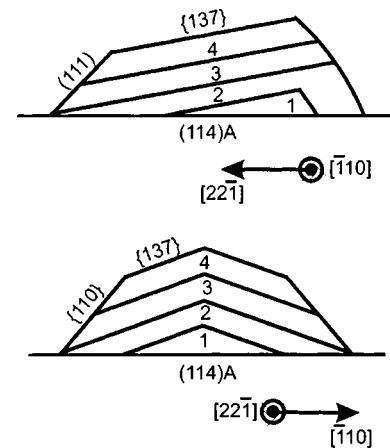


FIG. 5. Cross-section profiles of growing InAs island on GaAs(114)A. The cross-section planes are parallel to  $(\bar{1}10)$  and  $(22\bar{1})$ , respectively.

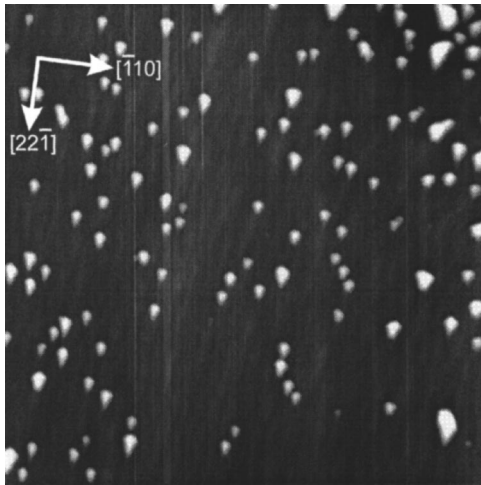


FIG. 6. Overview STM image of InAs islands on GaAs(114)A prepared at 430 °C. The image size is  $800 \times 800 \text{ nm}^2$ .

shape transition is probably quite general; it may be similarly applied for the growth of InAs QD's on GaAs(001) surfaces<sup>8,10</sup> or Ge QD's on Si(001),<sup>6,7</sup> although the detailed facets may be different due to different surface symmetry and composition.

It is noted that the critical diameter in our experiment is surprisingly small (12.3 nm) compared to other experimental results<sup>8–10</sup> including our own result (20 nm) discussed below. The low mobility of the adatoms, caused by low growth temperature, may play a role in establishing such a small critical base area. However, the fact that the critical base area is identical for all the islands indicates that the shape evolution still follows thermodynamics even at the low growth temperature. Considering that the strain energy is proportional to the square of the lattice mismatch and that larger strain leads to a smaller critical base area, the possible reason for the small critical base areas in our case may be found in the following: Due to the low growth temperature, In alloying is likely to be avoided, resulting in a maximum strain between the pure InAs QD's and the GaAs substrate as compared to alloyed  $\text{In}_x\text{Ga}_{1-x}\text{As}$  QD's. The evidence for alloying in uncapped InAs islands on GaAs has already been shown in experiments for growth temperatures above 420 °C.<sup>20</sup>

The above results only concern the small flat islands and some transition states. The islands are considered to be at the initial stage of QD growth. With further growth, the QD's will adopt their mature stage as discussed in the following.

### B. Mature stage

Figure 6 shows an overview STM image of InAs QD's grown on a GaAs(114)A substrate at 430 °C. There are many islands with regular shape and some larger islands with irregular shape. The majority QD's are actually much larger than the big islands in Fig. 1. The number density of the QD's is about  $1.8 \times 10^{10} \text{ cm}^{-2}$ , which is—according to our estimate—much lower than that for Fig. 1. This is caused by the higher growth temperature of 430 °C that increases the mobility of the adatoms on the wetting layer and leads to a

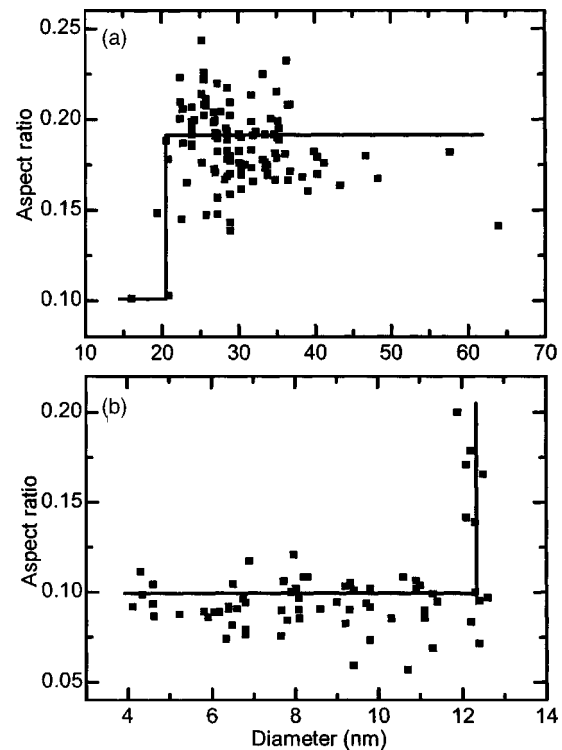


FIG. 7. Aspect ratios of InAs QD heights as a function of their diameters. The QD's are grown at (a) 430 °C and (b) 380 °C, respectively.

low nuclei density. The majority QD's are basically symmetric with respect to the  $(\bar{1}10)$  plane perpendicular to the surface, reflecting the symmetry of the substrate, similarly as for the QD's in Fig. 1.

To get further insight, the aspect ratios  $h/d$  are presented in Fig. 7(a) as a function of QD size (diameter  $d$ ) for the QD's grown at 430 °C. Here the bottom diameter  $d$  and the height  $h$  are defined in the same way as above. The aspect ratios  $h/d$  vs the island size (diameter  $d$ ) grown at 380 °C, as derived from Fig. 2, are shown in Fig. 7(b). The island sizes  $d$  are distributed between about 4 and 12 nm. When the size is smaller than 12.3 nm, the QD exhibits an aspect ratio of about 0.1. With increasing size, the aspect ratio remains the same, revealing a similar shape of the QD's. When the size exceeds 12.3 nm, the aspect ratio increases suddenly to about 0.20. This means that a shape transition from flat to steep occurs, as shown in Fig. 5, and the critical size for the shape transition is about 12.3 nm in this case. While in Fig. 7(a), most QD diameters are distributed between 20 and 50 nm with an average aspect ratio of  $\sim 0.20$ ; only very few QD's have diameters smaller than 20 nm and an aspect ratio of  $\sim 0.10$ . This means that the shape transition takes place at a critical size of about 20 nm in this case. In both cases, the typical aspect ratio is either 0.10 or 0.20, indicating that the QD's are of similar shape in both cases although their volumes are very different.

In Fig. 7(a), most QD's are in the steep, i.e., mature state. In addition, their critical size is much larger than that in Fig. 7(b). The small critical size in Fig. 7(b) is considered to be caused by pure InAs islands and a pure GaAs substrate due

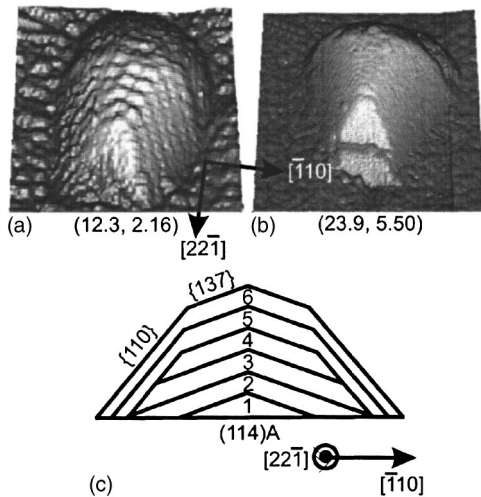


FIG. 8. 3D STM images of two mature InAs QD's on GaAs(114)A. The diameter and height (in units of nm) of the individual QD are given in brackets at the bottom of each image. The image sizes are (a)  $12.5 \times 12.5 \text{ nm}^2$ , and (b)  $29.0 \times 29.0 \text{ nm}^2$ . (c) Growth model; cut trough  $(2\bar{2}1)$ .

to the low growth temperature. Similarly, the large critical size in Fig. 7(a) is attributed to the high growth temperature, which favors intermixing of In and Ga, therefore reduces the effective lattice mismatch between substrate and QD's, and thus increases the critical size. In addition, for sizes larger than 35 nm in Fig. 7(a), the aspect ratio is decreased again. This means that either dislocations are incorporated or coalescence with a neighboring island takes place. We note that the absolute width of the size distribution of the larger QD's in Fig. 7(a) is larger than that of the small QD's in Fig. 7(b). This is contrary to some reports which found that the size distribution of larger QD's is sharper than that of small QD's.<sup>21,22</sup>

Furthermore, it is noted that the maximum relative deviation in aspect ratio is relatively large ( $\pm 25\%$ ) in both cases. For the small QD's we have discussed this already above in connection with Fig. 2. The deviation from the mean value seems to be a question of completion of the growing adlayers at the QD. The variation of aspect ratio for the large QD's [Fig. 7(a)] is not easy to understand. We think that mainly two factors are responsible, some variation in the degree of alloying and some measuring error in determining the diameters.

Whereas in Fig. 7(b), in which most islands are in the flat, initial state (before the shape transition), in Fig. 7(a) most QD's are in the steep, mature state (after the shape transition). In the mature state, the QD's have an average aspect ratio of 0.20, which is equal to the maximum shown in Fig. 7(b), meaning that they may have similar shapes. The 3D STM images for mature QD's in both cases are shown in Figs. 8(a) and 8(b); they have quite a different volume, but their shape is basically the same. A schematic model for the inner part of the QD was shown earlier in Figs. 4(c) and 5. Although the shape is the same, the overall construction of the outer part may be somewhat different as indicated in Fig. 8(c). In all models the top facet are noted as  $\{137\}$ . This is a

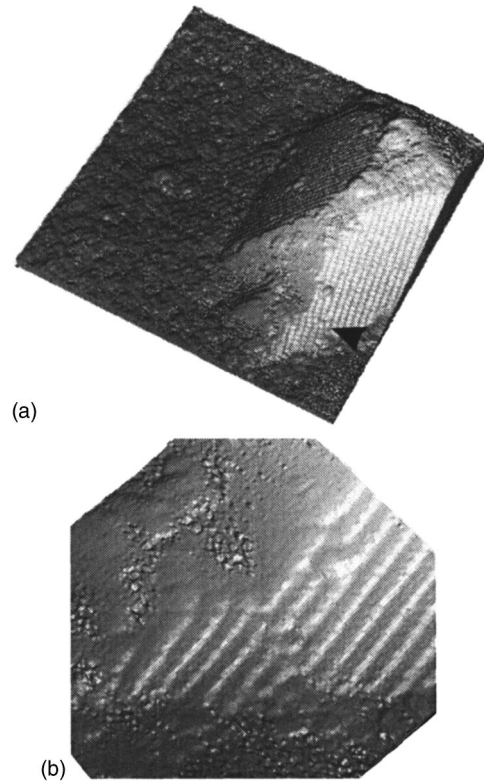


FIG. 9. (a) 3D STM image of InAs QD with a lattice defect. The size is  $40 \times 40 \text{ nm}^2$ . (b) Enlarged image of the defect.

subunit of  $\{2\ 5\ 11\}$  and transforms into the latter for large enough facets. So, strictly speaking, in Fig. 8(b) the top facets have become  $\{2\ 5\ 11\}A$ .

According to this analysis, the cross section of the InAs QD's in the mature stage is schematically sketched in Fig. 8(c). After formation of the mature QD's, the growth continues with simultaneously accommodating additional top and side facets so that the aspect ratio is kept constant at 0.20. During growth of mature QD's, their shape seems to stay the same until dislocations are incorporated at the edge of the islands. In fact, the larger QD's in the mature stage were found to exhibit slightly different shapes, i.e., the round part in the structure model shown in Fig. 4(c) is faceted in several, slightly varying combinations of  $\{110\}$ ,  $(111)A$ ,  $\{111\}B$ , and  $\{2\ 5\ 11\}A$  facets.<sup>19</sup> This multistructure shape seems to be a general property in the nanoworld.<sup>23</sup>

### C. Formation of dislocations

If a larger QD continues to grow, the strain in the QD will increase and consequently, to relieve the strain, dislocations may be incorporated, very likely at the edge of the QD. The incorporation of dislocations may change the shape of the QD. Figure 9(a) presents an atomically resolved 3D STM image of a larger island. The main part of the island is obviously the same as that in Fig. 8(b): two  $\{110\}$  facets, one  $(111)A$  facet, and a steep round region form at the side, and  $\{2\ 5\ 11\}A$  facets at the top.

Furthermore, an additional part, which looks like a small island, is attached to the main QD on the  $(111)A$  facet. In-

terestingly, on the (011) facet a lattice defect, marked by an arrow, occurs. The defect seems to separate the added from the main part. An enlarged image of the defect is shown in Fig. 9(b). The defect occurs probably in a  $\{111\}$  plane, which is consistent with the fact that InAs grows on GaAs(111) in the layer-by-layer mode with the incorporation of dislocations, i.e., a dislocation is easily formed in a  $\{111\}$  plane.<sup>24</sup> The defect may be caused by a lattice slip, with a slip direction in the  $\{111\}$  plane as derived from Fig. 9. The actual lattice distortion is related to the interface area between the wetting layer and the island, i.e., the base area of the QD. During growth the base area of the island increases. When it exceeds a critical size, a distorted bond may be broken, slip outwards to a suitable distance, and form another bond with an atom in the wetting layer, such that a dangling bond inside the island is created. The evolving structure is called an edge dislocation. One model of the lattice defect, lying on a  $\{110\}$  facet in a  $\{111\}$  plane, has already been described through a stacking fault mechanism.<sup>25,26</sup> A stacking fault is accompanied by an edge dislocation.

Fortunately, the dislocation, whose slip direction is parallel to the wetting layer, was observed also in our experiments for InAs QD's grown on GaAs(114)A and GaAs(113)A (not shown here). Such dislocations have been considered to be the reason that some QD's are elongated along the symmetric axis. The elongation decreases the aspect ratio for diameters larger than 36 nm as seen in Fig. 7(a). More dislocations may exist near to the interface between the wetting layer and islands, but we cannot look to the interface with our method.

Obviously, the occurrence of a dislocation affects the shape of the island, as can be seen from Fig. 9(a). The different slip direction of the dislocation determines which direction is preferred in growth because the dislocation effectively relaxes the elastic strain along its slip direction. Inversely, the slip direction of the possible dislocation should be also derived from the shape change. Figure 10(a) shows a STM image of some large islands. They are prepared by deposition of 0.33 nm InAs at 380 °C and then postannealing at 440 °C for 6 min to dissolve the small islands. Because these islands are much larger than the majority islands discussed above, even before the annealing (not shown here), they are very likely dislocated. The different shape of the islands, or their different elongation direction, indicates that there actually exist various slip directions of dislocations.

Also interesting is an island with an irregular shape, marked by an arrowhead in Fig. 10(a), whose enlarged image is shown in Fig. 10(b). It is not clear that a screw dislocation is really observed in Fig. 10(b), marked by "1." A screw dislocation has been observed more clearly on the InAs island grown on GaAs( $\bar{1}\bar{3}\bar{5}$ )B surfaces recently.<sup>26</sup> Generally, the crystal grows preferentially along the screw dislocation, but in Fig. 10(b), another preferential growth region, the step of another incomplete facet, exists on the same facet simultaneously, marked by "2." The interplay between the two preferential growth regions produces additional strain and actually blocks the continuous growth of the incomplete facet, so that the irregular shape is kept.

#### IV. CONCLUSION

InAs QD's grown by molecular beam epitaxy on GaAs(114)A substrates were studied by atomically resolved

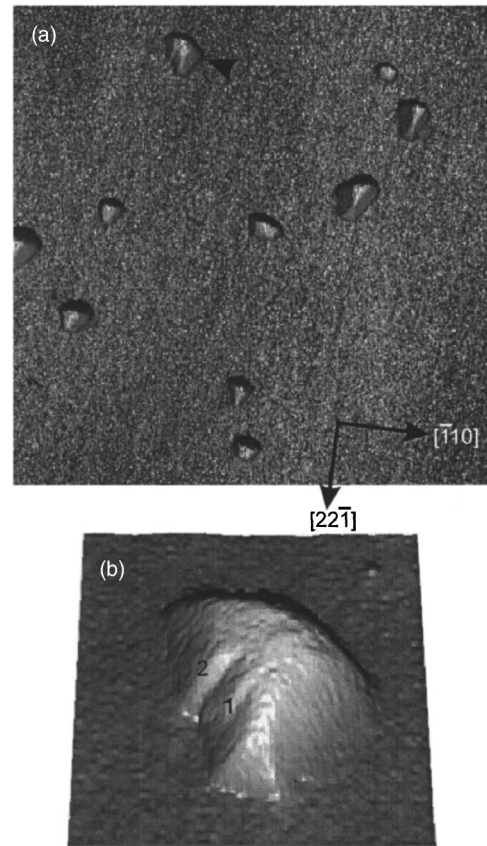


FIG. 10. (a) Overview 3D STM image of large InAs islands on GaAs(114)A. The size is  $500 \times 500$  nm<sup>2</sup>. (b) The enlarged image of the island with an irregular shape marked by an arrow head in (a). The size is  $64.3 \times 64.3$  nm<sup>2</sup>.

*in situ* STM. Two frozen-in QD distributions prepared at different temperatures were analyzed under the assumption, that QD's are depicted, which exhibit some variation in evolution mainly due to the statistics in nucleation. After nuclei formation, the QD's were found to grow first in a flat form with  $\{137\}$ -oriented facets and an aspect ratio of only 0.10. During the following growth, a shape transition from flat to steep occurs, the latter being characterized by  $\{110\}$  and (111)A facets and an aspect ratio of 0.20. An according growth model is proposed. We call the steep state "mature" since it basically remains for a large range of sizes. The shape transition occurs at a critical size of the diameter. Although the flat dots developing first reduce the strain, they are still strained. Therefore it is very plausible that at a given diameter this strain is again too large, so that the lateral growth is slowed down and the dot grows mainly vertically which results then in the shape transition. The critical diameter was found to be dependent on growth temperature, i.e., to be 12.3 nm at 380 °C and 20 nm at 430 °C, respectively. Arguments are given that the change in critical diameter is related to In and Ga alloying and the related change in induced strain: The small critical size (12.3 nm) at 380 °C is attributed to the pure InAs islands on top of the GaAs substrate because alloying does not occur at the low temperature. The

large QD's continue growing until dislocations are formed, and the shape is changed again. At this point probably both edge and screw dislocations were incorporated. An edge dislocation could be depicted here by STM on top of a facet. The detailed analysis for the InAs islands at initial growth indicates that the strain is localized in the bottom most few layers and decays quickly with increasing height. For the flat islands, both stable and metastable states are observed. Gen-

erally we conclude that the island shape derives mainly from thermodynamics rather than from kinetics.

#### ACKNOWLEDGMENTS

We thank G. Ertl for support, P. Geng for technical assistance, and M. Richard for the layout of the figures.

\*Author to whom correspondence should be addressed. Electronic address: jacobi@fhi-berlin.mpg.de

<sup>1</sup>D. Bimberg, M. Grundmann, and N. N. Ledentsov, *Quantum Dot Heterostructures* (Wiley, Chichester, New York, 1999).

<sup>2</sup>M. Grundmann, *Physica E (Amsterdam)* **5**, 167 (2000).

<sup>3</sup>*Semiconductor Quantum Dots*, edited by Y. Masumoto and T. Takagahara (Springer, Berlin, 2002).

<sup>4</sup>I. N. Stranski and L. Krastanow, *Sitzungsber. Akad. Wiss. Wien, Math.-Naturwiss. Kl., Abt. 2B* **146**, 797 (1937).

<sup>5</sup>A. Vailionis, B. Cho, G. Glass, P. Desjardins, D. G. Cahill, and J. E. Greene, *Phys. Rev. Lett.* **85**, 3672 (2000).

<sup>6</sup>G. M-Ribeiro, A. M. Bratkovski, T. I. Kamins, D. A. A. Ohlberg, and R. S. Williams, *Science* **279**, 353 (1998).

<sup>7</sup>F. M. Ross, R. M. Tromp, and M. C. Reuter, *Science* **286**, 1931 (1999).

<sup>8</sup>H. Saito, K. Nishi, and S. Sugou, *Appl. Phys. Lett.* **74**, 1224 (1999).

<sup>9</sup>I. Mukhametzhanov, Z. Wei, R. Heitz, and A. Madhukar, *Appl. Phys. Lett.* **75**, 85 (1999).

<sup>10</sup>H. Lee, R. Lowe-Webb, W. Yang, and P. C. Sercel, *Appl. Phys. Lett.* **72**, 812 (1998).

<sup>11</sup>J. Márquez, L. Geelhaar, and K. Jacobi, *Appl. Phys. Lett.* **78**, 2309 (2001).

<sup>12</sup>J. Porsche, A. Ruf, M. Geijer, and F. Scholz, *J. Cryst. Growth* **195**, 591 (1998).

<sup>13</sup>J. Márquez, P. Kratzer, L. Geelhaar, K. Jacobi, and M. Scheffler, *Phys. Rev. Lett.* **86**, 115 (2001).

<sup>14</sup>J. Márquez, P. Kratzer, and K. Jacobi, *J. Appl. Phys.* **95**, 7645 (2004).

<sup>15</sup>S. Shimomura, K. Shinohara, T. Kitada, S. Hiyamizu, Y. Tsuda, N. Sano, A. Adachi, and Y. Okamoto, *J. Vac. Sci. Technol. B* **13**, 696 (1995).

<sup>16</sup>S. Kiravittaya, R. Songmuang, P. Changmuang, S. Sopitpan, S. Ratanathamaphan, M. Sawadsaringkarn, and S. Panyakeow, *J. Cryst. Growth* **227–228**, 1010 (2001).

<sup>17</sup>P. Geng, J. Márquez, L. Geelhaar, J. Platen, C. Setzer, and K. Jacobi, *Rev. Sci. Instrum.* **71**, 504 (2000).

<sup>18</sup>K. Jacobi, *Prog. Surf. Sci.* **71**, 185 (2003).

<sup>19</sup>M. C. Xu, Y. Temko, T. Suzuki, and K. Jacobi, *Appl. Phys. Lett.* **84**, 2283 (2004).

<sup>20</sup>P. B. Joyce, T. J. Krzyzewski, G. R. Bell, B. A. Joyce, and T. S. Jones, *Phys. Rev. B* **58**, R15 981 (1998).

<sup>21</sup>F. M. Ross, J. Tersoff, and R. M. Tromp, *Phys. Rev. Lett.* **80**, 984 (1998).

<sup>22</sup>G. Costantini, C. Manzano, R. Songmuang, O. G. Schmidt, and K. Kern, *Appl. Phys. Lett.* **82**, 3194 (2003).

<sup>23</sup>M. J. Yacaman, J. A. Ascencio, H. B. Liu, and J. G-Torresdey, *J. Vac. Sci. Technol. B* **19**, 1091 (2001).

<sup>24</sup>H. Yamaguchi, M. R. Fahy, and B. A. Joyce, *Appl. Phys. Lett.* **69**, 776 (1996).

<sup>25</sup>N. Wang, K. K. Fung, and I. K. Sou, *Appl. Phys. Lett.* **77**, 2846 (2000).

<sup>26</sup>T. Suzuki, Y. Temko, M. C. Xu, and K. Jacobi, *Phys. Rev. B* **69**, 235302 (2004).